Drew University
College of Liberal Arts

Investigating the Effects of pH and Salt Concentration on Substrate Inhibition of Yeast Aldo-Keto Reductase 163

A Thesis in Biochemistry and Molecular Biology

By

Joel Asabi Moses

Submitted in Partial Fulfillment
of the Requirements
for the Degree of
Bachelor in Science
With Specialized Honors in Biochemistry and Molecular Biology

May 2024

Abstract

Aldo-keto reductases (AKRs) are a broad superfamily of NADPH-dependent oxidoreductases capable of catalyzing the reduction of many carbonyl compounds into alcohols in living systems and industrial settings. Most studied AKRs exhibit substrate saturation where they experience typical Michaelis-Menten kinetics with their substrates. However, a novel AKR isolated from ancient amber called AKR 163 experiences a phenomenon called substrate inhibition in the presence of electron withdrawing substrates such as ethyl 4-chloroacetoacetate (E4ClAA). This characteristic is often undesirable biologically and industrially since it leads to poor product yields. Unfortunately, there are few studies that aim to alleviate substrate inhibition despite its disadvantages. For these reasons, researchers used AKR 163 as a model enzyme to test the effects of pH on substrate inhibition. They found that decreasing pH reduced substrate inhibition. However, these studies used two types of buffers to gather data from a wide range of pHs, which could have led to inconsistent results. Similarly, researchers have also tested the effects of exogenous salt ions on substrate inhibition and found that adding salt decreases inhibition. Given the successes and shortcomings of these researchers, I combined these ideas to observe and explain the effects of salt ions and pH changes together on substrate inhibition using an ACES buffer system and E4ClAA as the substrate. My results confirm that lowering pH and adding salt decrease substrate inhibition individually. Furthermore, the lowest pH trial (pH 6) with 1M NaCl showed almost no signs of inhibition with up to 6 mM of substrate, and the plot resembled a Michaelis-Menten curve. These results indicate that substrate inhibition can be almost completely inhibited under those conditions.

Table of Contents

List of Figures and Tables

Introduction

Overview: Enzymes

Multitudes of chemical reactions are carried out in the world around us to sustain life. These reactions have varying rates - some occur instantaneously while others take a long time. Biologically, making slower reactions occur quicker is essential for metabolism and other cellular processes. Industrially, speeding up sluggish reactions is crucial to increase the yield of vital products. For these reasons, humans and other living organisms make use of catalysts for survival. Catalysts are substances capable of increasing the rate of reactions without being consumed or changing their equilibrium (Cooper 2000). They are capable of doing this action by decreasing the energy required to convert reactant molecules to products while stabilizing the reaction's transition state (Figure 1).

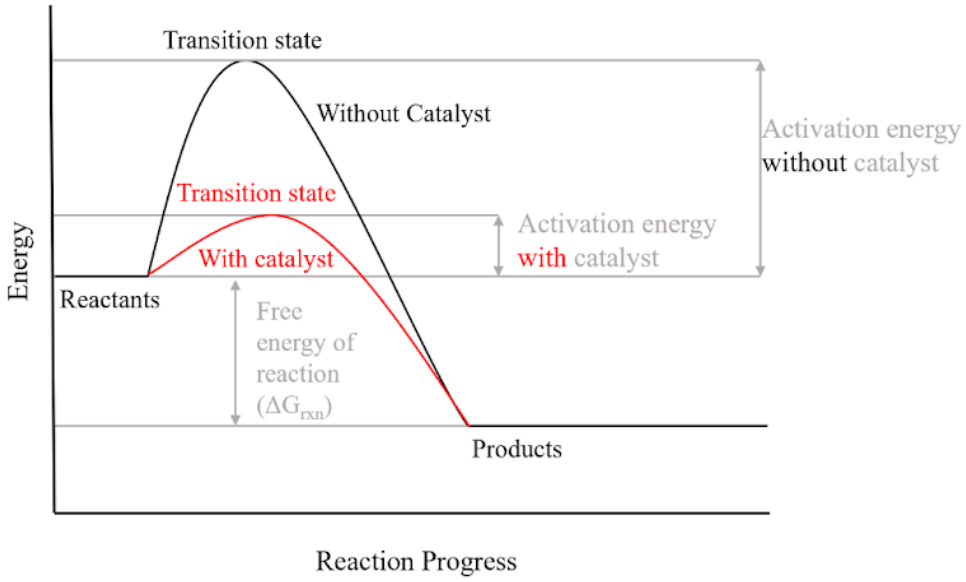

Figure 1. A typical catalyst reaction coordinate diagram. This plot shows the energy needed to convert reactants into products for catalytic (red) and non-catalytic (black) reactions. With catalysts, the energy needed to generate products (activation energy) is smaller than without the catalyst. Furthermore, the energy required to maintain the transition state is lower in the presence of a catalyst. The free energy of the reaction (ΔG_{rxn}) is unaffected by catalysts.

Enzymes are biological catalysts (usually proteins) within living organisms' cells (Liu et al. 2007). They work similarly to other catalysts by decreasing the activation energy of the reaction and stabilizing the transition state (Lewis and Stone. 2023). However, their mechanism is slightly different. When an enzyme binds the reactant (or substrate), it forms a low-energy enzyme-substrate complex (Figure 2A and B). Once formed, the enzyme-substrate complex enters a relatively high energy transition state. During this state, the substrate is converted to a product, yielding a stable, low-energy enzyme-product complex. Ultimately, the product is removed from the enzyme's binding site when the reaction is complete. By performing these feats, enzymes convert substrates to products at high velocities and efficiency (Figure 2B).

A

$$E+S \rightleftharpoons ES \rightleftharpoons ES^* \rightleftharpoons EP \rightleftharpoons E+P$$

B

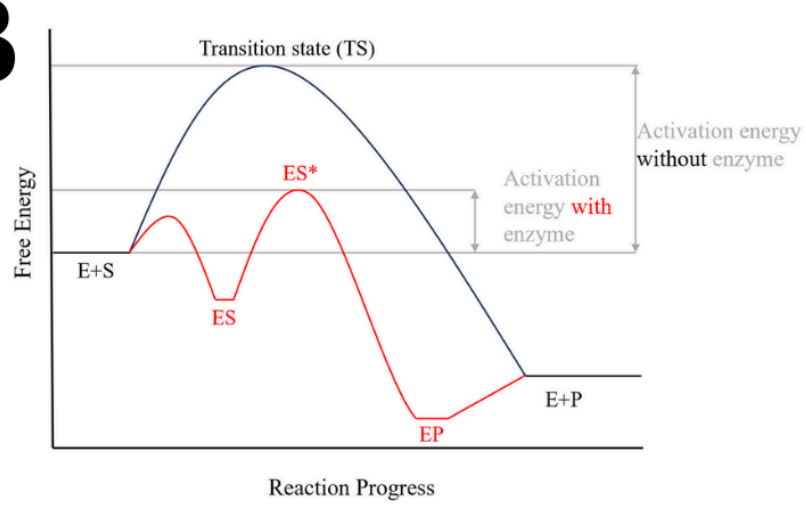

Figure 2. General mechanism of enzyme catalysis. E represents the enzyme, S signifies the substrate, and P is the product. (A) Enzyme reaction coordinate diagram. When the enzyme and substrate are physically close (E+S), they bind, forming an enzyme-substrate complex (ES). They then form a high energy transition state (ES*), and the product is made (EP). Finally, the product is released from the enzyme (E+P). (B) The reaction coordinate diagram corresponding to 2A. The free enzyme utilizes many non-covalent interactions to bind the substrate and form a low-energy ES complex. The ES complex progresses into the high-energy ES* state, where the substrate is converted to a product, forming a low-energy EP. Ultimately, the product is released after breaking non-covalent interactions with the enzyme.

Despite similarities in the general function of enzymes, these biological catalysts can perform various tasks and are separated into six main groups based on the substrates they act upon (Lewis and Stone. 2023). These groups are oxidoreductases, transferases, hydrolases, lyases, isomerases, and ligases. Due to their ability to catalyze multiple reactions, each of the six general groups of enzymes is found in all living organisms. (Singh et al. 2016). This reason alone provides a considerable incentive to study their applications. However, besides their biological importance, humans have incorporated enzymes into industrial uses (Schmid et al. 2002). From making food products to drug development, enzymes are prominent tools in varying industries due to their cheapness and versatility (Ranjbari et al. 2018). Furthermore, unlike many chemical catalysts, enzymes are renewable, biodegradable, generate low amounts of waste, and can act in milder conditions (Bell et al. 2021). These additional reasons provide a further motive for studying the mechanisms of enzyme catalysis.

Industrial Uses of Enzymes

For centuries, humans used enzymes to catalyze the production of various foodstuffs (Singh et al. 2016). The earliest uses of enzymes stem from the production of alcoholic beverages from sugars as early as 7000 BC (McGovern et al. 2004). These reactions usually utilized amylases, a subgroup of hydrolases capable of breaking down complex sugars (Souza and Magalhães 2010; Raveendran et al. 2018). As time passed, enzymes started to have broader industrial applications. In these settings, microbial enzymes are used over plant or animal enzymes due to their genetic stability (Rao et al. 1998; Mohapatra et al. 2003). Their availability also provides a cheap and effective way to synthesize large amounts of goods.

During the past few decades, advancements in DNA recombinant technologies and protein engineering have allowed the production of more diverse and catalytically productive enzymes (Singh et al. 2016). These developments mean that the industrial use of enzymes is growing; increasing the efficiency of enzymatic technologies is becoming more important in the modern age. For example, an engineered version of the oxidoreductase known as cytochrome P450 could synthesize (2S-6S)-hydroxynorketamine at high yields (Bokel et al. 2020). This molecule is a critical intermediate for the antidepressant drug esketamine, more commonly known as Spravato. Another example would be ω-transaminase. This enzyme is a transferase used to synthesize or modify chiral amine groups for drug synthesis (Patil et al. 2018). However, its binding site naturally only fits smaller chemical groups (Han et al. 2015). Researchers have modified it to incorporate larger substrate molecules. Both enzymes showcase important aspects of pharmaceutical synthesis - efficiency and stereoselectivity.

From 7000 BC to today, enzymes have become more commonplace (Singh et al. 2016). Globally, hydrolases produce the most revenue out of all the six main classes of enzymes (Espina et al. 2021). Subclasses of hydrolases like proteases and amylases are often used to make food products, develop therapies, and create textiles (Adler-Nissen 2007). Papain, a protease isolated from the papaya plant, has potential as a treatment for obesity (Kang et al. 2021). Additionally, it's used in the food industry as a meat tenderizer while also having other pharmaceutical uses. Oxidoreductases are the second-highest revenue generators in the world (Espina et al. 2021). However, despite their prevalence, oxidoreductases are not usually utilized for the bulk production of chemicals due to a lack of selectivity and efficiency issues (Martínez et al. 2017).

Developing and implementing methodologies to deal with these problems would open new doors for chemical synthesis.

Oxidoreductases

Oxidoreductases are one of the six main groups of enzymes (Lewis and Stone 2023). As their name suggests, they catalyze the oxidation or reduction of substrates via hydride or electron transfer, usually with the help from a cofactor (Singh et al. 2016). Cofactors help catalysis by stabilizing the enzyme, participating in the chemical reactions, or assisting with substrate binding (Robinson et al. 1997; Schwarz et al. 2009). Enzymes such as alcohol dehydrogenase (ADH) utilize NAD^+ or NADH to oxidize or reduce substrates (Sicsic et al. 1984). ADH oxidizes alcohol using NAD^+ as an electron donor. Enzymes like isocitrate dehydrogenase use $NADP^+$ (Imada et al. 2017). Specifically, this enzyme oxidizes isocitrate to α-ketoglutarate in the citric acid cycle. Flavin-containing enzymes include glucose oxidase, which catalyzes the oxidation of substrates using Flavin Adenine Dinucleotide (FAD) (Chen et al. 2021). Enzymes such as Cytochrome P450 can use metal ions as cofactors (Dydio et al. 2017). This enzyme uses metals or NADH to help substrate binding and facilitate oxidation.

Oxidoreductases can be further subdivided into groups such as peroxidases, reductases, dehydrogenases, oxygenases, and many more (Monti et al. 2011). Each of these subclasses have important biological functions. For example, catalase is a peroxidase capable of reducing reactive oxygen species (ROS); if downregulated, cells can suffer from various types of damage (Min et al. 2010). In addition to their biological roles, these enzymes often have industrial

potential. This feature also applies to catalase, which is often used industrially to produce clothing and textiles (Espina et al. 2021). Unfortunately, these enzymes often face many restrictions that limit their use (Martínez et al. 2017). For example, some are unable to function with large amounts of substrates. However, discovering novel enzymes or engineering existing enzymes remain the most optimal methods to solve these problems.

In the past few decades, many novel aldo-keto reductases with industrial applications were discovered. For example, three Lodderomyces *elongisporus* Aldo-Keto reductases (LEAKRs) were isolated and engineered to efficiently and stereospecifically reduce ethyl 4-chloroacetoacetate (Ning et al. 2014). Other researchers isolated another novel aldo-keto reductase capable of producing 1,3-butanediol, an intermediate of many polymers including polyethylene terephthalate and polyurethane (Kim et al. 2017). Biologically, AKRs are involved in many cellular processes and/or diseases. These include inflammatory regulation in several organs including the eyes (Chang et al. 2016), heart (Ramana et al. 2006), and kidneys (Yagihashi et al. 2010). These and other discoveries have shown the promise of studying the mechanisms and applications of aldo-keto reductases.

Aldo-Keto reductases

Aldo-keto reductases (AKRs) are a superfamily of NADPH-dependent oxidoreductases - they convert carbonyl groups to alcohols in the presence of NADPH (Sanli et al. 2003). AKRs are found in multiple species and are involved in many human diseases (Penning 2015). They

also have broad specificity and perform stereoselective catalysis, which makes them excellent for industrial applications (Figure 3). Some can even catalyze the oxidation of alcohols to carbonyls using $NADP^+$ as the cofactor, contributing to the wide range of reactions they can catalyze. Due to their biological and industrial relevance, identifying and characterizing AKRs is crucial to understand their functionality.

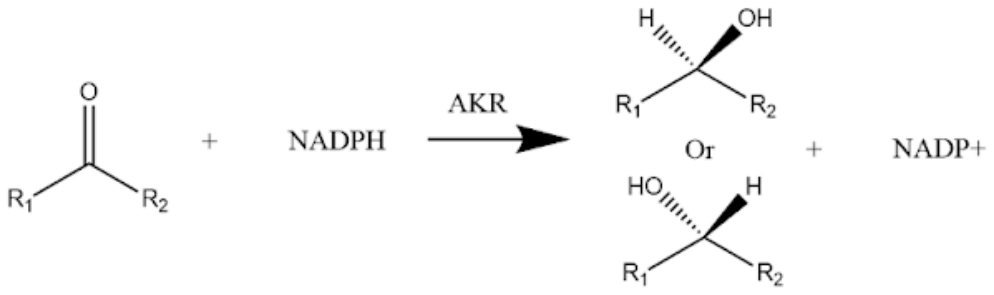

Figure 3. **Stereoselective reduction scheme of Aldo-keto reductases.** The enzyme binds to NADPH and the carbonyl substrate to produce alcohol and $NADP^+$.

Homology and Structure of Aldo-Keto Reductases

AKRs are found in all phyla on the planet (Penning et al. 2015). Naturally, this means the the superfamily consists of many diverse members - there are over 190 proteins categorized into 16 families (AKR 1 to AKR 16). However, despite their vast numbers, they share many conserved traits. For instance, most AKRs are soluble and usually monomeric proteins (Sanli et al. 2003). The amino acids of these proteins adopt a $(\beta/\alpha)_8$ motif, also referred to as a Triose phosphate isomerase (TIM) barrel. This motif describes the general structure of AKRs - they form eight parallel β sheets surrounded by eight α helices (Barski et al. 2008). Proteins with this structural feature usually have catalytic functionality on the C-terminal face of the central

β-barrel (Vez et al. 2003). AKRs are no exception. In AKRs, behind these TIM barrels are three loops that govern substrate specificity - these are commonly called loops A, B, and C (Ellis 2002). Due to these and other features, all AKRs lack flavin or metal cofactors and utilize NADPH to reduce carbonyl groups into alcohols instead. (Barski et al. 2008). However, a few AKRs, such as AKR 1C12 (Ikeda et al. 1999) and AKR2B5 (Kratzer et al. 2006), can catalyze reactions with NADH.

The cofactor binding domain in AKRs is also conserved (Penning 2015). When bound, NADPH is oriented to allow the nicotinamide ring to face upward (Figure 4). Four conserved amino acids in the cofactor binding domain interact with the nicotinamide ring of NADPH and facilitate its hydride transfer (Ellis 2002). These residues are tyrosine (Tyr), histidine (His), aspartic acid (Asp), and lysine (Lys). The phosphate group on the opposite end of the NADPH molecule binds to other amino acids, such as serine and arginine, through electrostatic interactions, which allows the compound to stay in place (Ma et al. 2000). This tight cofactor binding mechanism is crucial to lowering the energy needed for the substrate to achieve its transition state (Grimshaw 1992). It also indicates that AKRs do not need to bind substrates tightly to function, meaning these enzymes can act on multiple types of carbonyl substrates (Barski et al. 2008).

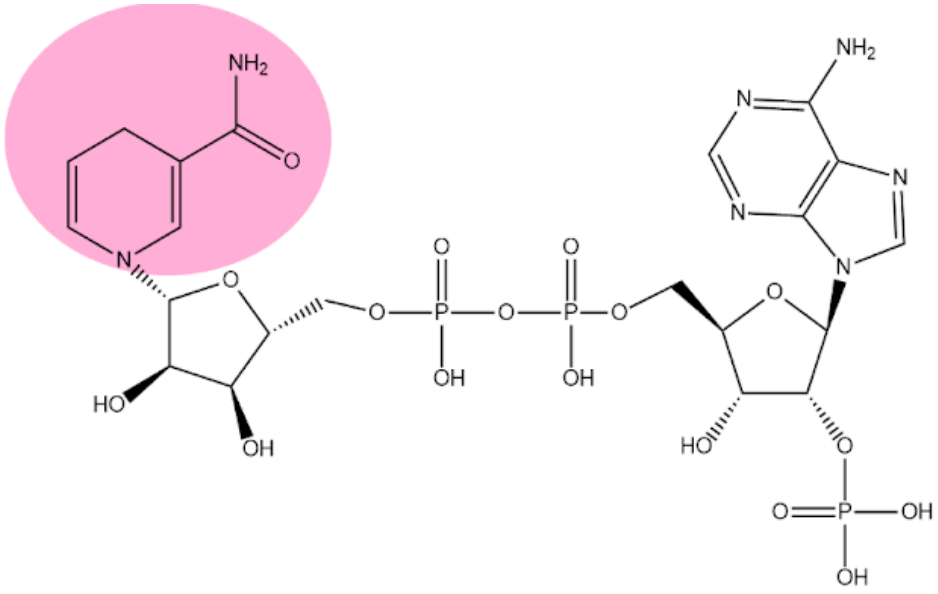

Figure 4. Structure of NADPH. The highlighted portion is the nicotinamide ring, which is responsible for catalysis. The 2' phosphate group on the other end is responsible for the molecule's tight binding to the enzyme.

Catalytic Mechanism of Aldo-Keto Reductases

Mechanistically, aldo-keto reductases follow a bi-bi reaction mechanism - NADPH and the carbonyl compound act as two substrates, and $NADP^+$ and the resulting alcohol are the two products (Jez et al. 1997). The enzyme uses NADPH to catalyze a hydride transfer to the carbonyl compound, reducing it. Due to this feature, AKRs follow an ordered binding mechanism where the NADPH binds the enzyme first and leaves last. The reduction aspect is due to a pro-R hydride transfer from NADPH to the substrate (Kratzer et al. 2006). The conserved His is responsible for this characteristic, which dictates the stereoselectivity of AKRs (Bohren et al. 1994).

For catalysis to occur in AKRs, the conserved tyrosine residue acts as a general acid/base that relays protons to other residues in the active site (Grimshaw et al. 1995). While the pKa value of Tyr's side chain is normally above 10, it is lowered when hydrogen bonded to the conserved Lys residue (Schlegel et al. 1998). This amino acid can bind the conserved Asp through similar electrostatic interactions. The altered pKa of Tyr allows for catalysis to occur via the push-pull mechanism.

The push-pull mechanism refers to a catalytic chemical reaction where electron-rich and electron-deficient groups interact. (Jencks 1969; Polgár 1987). On one hand, an electron-donating amino acid can act as a base to remove a proton from the substrate, resulting in oxidation. This residue is termed the push element. On the other hand, an electron-withdrawing amino acid can act as an acid to facilitate reduction. This residue is termed the pull element. In the reduction (forward) reaction of AKRs, NADPH donates its hydride ion to the carbonyl substrate, forming the alcohol group (Penning 2015). Tyr acts as the pull element by donating a proton to the substrate (Figure 5). For some AKRs, such as AKR 1C9, His gives Tyr this feature (Penning 2015). In the oxidation (reverse) direction, Lys reduces Tyr, making it a push element. The Tyr residue can act as a base to gain a proton from the alcohol substrate. This reaction causes a hydride transfer from the substrate back to the oxidized cofactor.

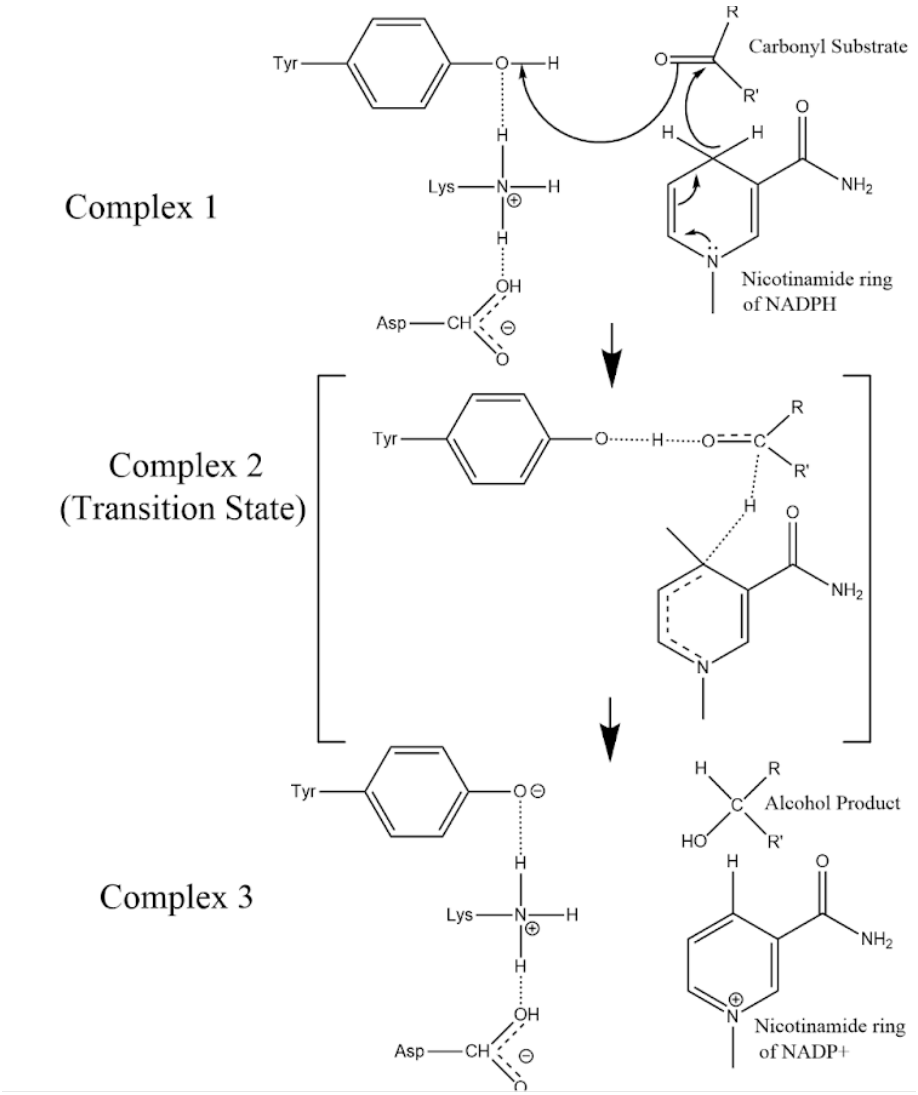

Figure 5. General reduction mechanism of AKRs. Complex 1 shows the hydride transfer from the nicotinamide ring of NADPH to the substrate. Simultaneously, the protonated tyrosine donates a hydrogen atom to the substrate. Complex 2 shows the transition state involving the tyrosine residue, the carbonyl substrate, and the nicotinamide ring. Complex 3 shows the reduced alcohol product, the oxidized $NADP^+$, and the oxidized tyrosine. Adapted from Barski et al. 2008 and Portadin 2023.

Aldo-Keto Reductases in Humans

In living organisms, most AKRs mainly perform reduction reactions due to the prevalence of NADPH over $NADP^+$ in metabolic cells (Pollak et al. 2007) and their high affinity for NADPH (Barski et al. 2008). This feature also applies to human AKRs (Penning et al. 2018). These AKRs participate in vital reactions and their dysregulation often leads to diseases (Chen and Zhang 2012).

Currently, there are 15 known human AKR isoforms from the AKR 1, AKR 6, and AKR 7 families (Penning 2015). These AKRs are pivotal in drug detoxification, metabolism, and other cellular reactions. When overexpressed or underexpressed, these enzymes can cause immense changes to cellular processes. For instance, aldehyde reductase (AKR1A1) participates in the metabolism of many chemotherapeutic drugs (Chen and Zhang 2012). It is also implicated in reducing steatosis, alcoholic liver damage, and fibrosis (Lan et al. 2022). When overexpressed, AKR1A1 may also protect lung epithelial tissue from toxic polycyclic aromatic organic compounds (Abedin et al. 2011). Steroid 5β-reductase (AKR1D1) reduces bile acid intermediates in the liver (Chen et al. 2015). When this enzyme is underexpressed, it results in liver dysfunction (Lemonade et al. 2003).

When overexpression results in negative health consequences, enzyme inhibitors are employed to alleviate disease (Penning 2015). The most studied human AKR, AKR1B1, reduces glucose into another sugar, sorbitol (Chen and Zhang 2012). Due to its function, this enzyme is involved in diabetes and is the target of many drugs (Gabbay et al. 1975). Inhibitors such as

Sorbinil, Tolrestat, and others have been tested to treat symptoms of diabetes (Penning 2015). Cases like these show that studying inhibitors is crucial to understanding their effects on diseases.

The Potential of Aldo-Keto Reductases in Industry

While AKRs are relevant biologically, they are underutilized in industry. However, due to the diverse amounts of substrates they catalyze, these enzymes have the potential to be industrially prominent. Some AKRs have avoided being overlooked such as AKR-IA (Pei et al. 2022). This artificial enzyme is used to synthesize an intermediate that can be used to produce the antidepressant drug duloxetine. However, this enzyme also shows some of the challenges associated with aldo-keto reductases; it is unstable and challenging to obtain. Due to limitations like these, modifying AKRs is also relevant to increase their catalytic abilities.

Another solution is using novel AKRs by identifying or genetically engineering them. For example, AKR 3-2-9 is a novel AKR that produces (*S*)-*N*, *N*-dimethyl-3-hydroxy-3-(2-thienyl)-1-propanamine, another intermediate of the drug duloxetine (Pei et al. 2020). This enzyme was stable, had a large optimal pH range, and functioned in many solvents. Another novel AKR called LEK catalyzes the production of ethyl (R)-4-chloro-3-hydroxybutyrate, an intermediate for many drugs including atorvastatin calcium and macrolide A (Wang et al. 2014). This enzyme had high product yields and a relatively broad optimal pH range. Given the success of these novel AKRs in catalyzing industrially relevant intermediates, the Cassano lab has also purified and characterized a novel enzyme, AKR 163 (Akbary et al.

2023). However, this enzyme is susceptible to substrate inhibition, a kinetic phenomenon that usually does not occur in other AKRs (Penning 2015). Overcoming such a drawback would be cardinal for the industrial success of this enzyme or enzymes homologous to it.

Aldo-Keto Reductase: Michaelis-Menten Kinetics

Most subsets within the AKR superfamily exhibit substrate saturation (Figure 6A), where the enzymatic activity increases with elevating substrate concentration (Penning 2015). This feature means that as the concentration of substrate increases, the velocity increases until it reaches a theoretical maximum value, V_{max} (Johnson and Goody 2011). In 1913, scientists observed and tested this phenomenon for the first time, making inferences about the nature of enzymes. The researchers, namely Leonor Michaelis and Maud Leonora Menten, quantified different aspects of enzymology; they identified a value that indicates the concentration of substrate required to reach ½ of V_{max} named the Michaelis constant (K_m). By combining quantitative and qualitative experimental data, they posterized the Michaelis-Menten equation which showed the relationship between different characteristics of enzymes (Figure 6B). Understanding this equation is key to understanding the mechanism of many enzymes.

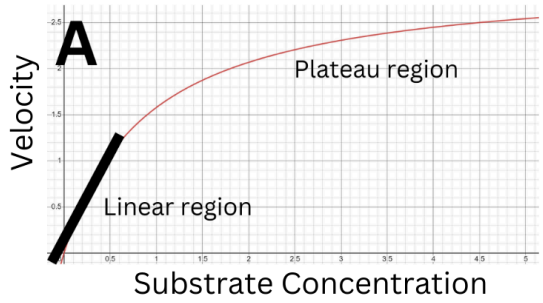

B

$$Velocity = \frac{V_{max}[S]}{K_m + [S]}$$

Figure 6. A method to analyze enzymatic kinetic data: the Michaelis-Menten curve and equation. (A) A typical substrate saturation (Michaelis-Menten) curve. Low substrate concentrations indicate the linear region, where the variables can be related to each other using the equation of the line: y=mx+b. In this region, as substrate concentration increases, reaction velocity increases proportionately. Higher substrate concentrations show the plateau region or dynamic range. The equation of the line is no longer applicable since substrate concentration and velocity are no longer proportional. However, the Michaelis-Menten equation can be used instead. (B) The modern version of the Michaelis-Menten equation. The velocity depends on maximum velocity (V_{max}), substrate concentration ([S]), and Michaelis-Menten constant (K_m).

Generally, in an enzymatic reaction, the enzyme and substrate come together to form a complex that produces products (Blaber 2021). Each step of this mechanism has a specific rate associated with it (Figure 7)

$$E+S \underset{k_{-1}}{\overset{k_1}{\rightleftharpoons}} ES \underset{k_{-2}}{\overset{k_2}{\rightleftharpoons}} E+P$$

Figure 7. General reaction mechanism of an enzyme. Where E represents the enzyme, S represents the substrate, and P represents the products. The rates of association (k_1 and k_2) and the rates of dissociation (k_{-1} and k_{-2}) are also shown.

The Michaelis-Menten equation operates under five different assumptions (Blaber 2021). The first assumption is that at the start of catalysis, no product is present. Therefore, the rate of E+P forming ES (k_{-2}) is negligible (Figure 8).

Figure 8. The enzymatic mechanism with the first assumption. The first assumption shows that k_{-2} is negligible.

The second assumption utilizes the steady-state mechanism identified by Briggs and Haldane (Cornish-Bowden 2013). This mechanism is based on the assumption that the rate of formation of ES is equal to its rate of breakdown. Therefore, the concentration of intermediates of the enzyme-catalyzed reactions remains constant over time. The third assumption requires the concentration of substrate [S] to be much higher than the concentration of the enzyme [E] (Blaber 2021). One enzyme can act on many different substrates, therefore [ES] is much lower than the [S]. In a short time, [S] is constant since a negligible amount of it forms ES. The fourth assumption requires that only the initial velocity (V_0) is observed since assumption one requires the amount of products to be zero and assumption three is only true at relatively short intervals of time. The final assumption is that the total amount of enzyme ($[E]_{total}$) is equal to [E] + [ES].

To derive the Michaelis-Menten equation, finding and relating the rate of formation and breakdown of ES is necessary according to the second assumption. The formation of ES would rely on the production of ES from E+S and the reverse of E+P. This would lead to

$$Rate\ of\ ES\ formation\ =\ k_1[E][S]\ +\ k_{-2}[E\ +\ P] \tag{1}$$

However, assumption one states that we can ignore the rate of E+P forming ES. Therefore, the modified equation would be

$$Rate\ of\ ES\ formation\ =\ k_1[E][S] \tag{2}$$

Assumption five states that $[E]_{total} = [E] + [ES]$. Therefore, [E] can be replaced with $[E]_{total} - [ES]$.

$$Rate\ of\ ES\ formation\ =\ k_1([E]_{total} - [ES])[S] \tag{3}$$

According to assumption two (steady-state assumption), the rate of ES breakdown involves the rate of product formation and product dissociation. These rates are equal.

$$Rate\ of\ ES\ breakdown = k_{-1}[ES]\ + k_2[ES]$$

$$Rate\ of\ ES\ breakdown =\ (k_{-1} + k_2)[ES] \tag{4}$$

$$Rate\ of\ breakdown = Rate\ of\ formation$$

$$(k_{-1} + k_2)[ES] = k_1([E]_{total} - [ES])[S]$$

(5)

Rearranging this equation to find the rate constants leads to the mathematical definition of the Michaelis-Menten constant (K_m).

$$\frac{([E]_{total} - [ES])[S]}{[ES]} = \frac{(k_{-1} + k_2)}{k_{-1}}$$

(6)

$$\frac{[E]_{total}[S]}{[ES]} - [S] = \frac{(k_{-1} + k_2)}{k_{-1}}$$

(7)

$$\frac{[E]_{total}[S]}{[ES]} - [S] = K_m = \frac{(k_{-1} + k_2)}{k_{-1}}$$

(8)

The velocity of an enzymatic reaction at any moment would be equal to the rate of formation of products from ES (Equation 9). Solving for ES and utilizing this feature would lead to a preliminary version of the Michaelis-Menten equation after multiplying both sides by k_2 (Equation 11).

$$V = k_2[ES]$$

(9)

$$[ES] = \frac{[E]_{total}[S]}{(K_m + [S])}$$

(10)

$$k_2[ES] = k_2 \frac{[E]_{total}[S]}{(K_m+[S])}$$

$$\therefore V = k_2 \frac{[E]_{total}[S]}{(K_m+[S])}$$

(11)

Theoretically, the maximum velocity (V_{max}) would be achieved when the [ES] being converted to products is equal to $[E]_{total}$ (Equation 12). This observation gives the modern Michaelis-Menten equation (Equation 13).

$$V_{max} = k_2[E]_{total}$$

(12)

$$\therefore V = \frac{V_{max}[S]}{(K_m+[S])}$$

(13)

Most AKRs exhibit substrate saturation and utilize this type of enzymatic kinetics. However, enzymes such as Aldo-Keto reductase 163 do not under specific conditions.

Aldo-Keto Reductase 163: Substrate Inhibition

Aldo-keto reductase 163 is a yeast AKR isolated from ancient amber (Akbary et al. 2023). Like other members of the superfamily, it catalyzes the reduction of carbonyl compounds to alcohols. Dr. Adam Cassano identified that this enzyme shared 98.7% of its amino acid sequence with an enzyme called YDL124W from *Saccharomyces* cerevisiae S288C. Previous studies with YDL124W indicate that it exhibits substrate saturation (Jung et al. 2010). However,

despite their homology, AKR 163 experiences a different type of kinetic characteristic in the presence of substrates with electron-withdrawing groups (Akbary et al. 2023).

Substrate inhibition refers to the kinetic phenomenon where the velocity of a reaction rises to a maximum and subsequently decreases as substrate concentration increases (Yoshino and Murakami 2015, Figure 9). It is the most common derivation of Michaelis-Menten kinetics and occurs in 25% of enzymes (Kokkonen et al. 2021) and only a handful of other AKRs (Yamamoto and Wilson 2013). This prevalence and its presence in regulatory enzymes suggest that this mechanism is biologically relevant and not a pathology (Reed et al. 2010). For example, the glycolytic enzyme phosphofructokinase is inhibited by high concentrations of ATP. However, despite its relevance, it is still understudied. Studying its mechanism of action can help determine ways to alleviate it in an industrial or laboratory setting.

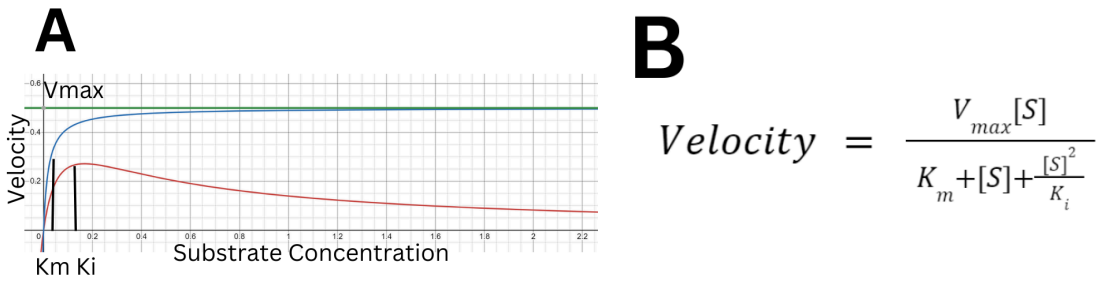

Figure 9. A deviation from Michaelis-Menten kinetics - substrate inhibition. (A) A typical substrate inhibition curve (red). The reaction velocity initially increases to a maximum before decreasing to zero or a non zero asymptote. The Michaelis-Menten constant (K_m) represents the minimum concentration required to reach a rate of ½ the maximum velocity (V_{max}) (green) while the inhibition constant (K_i) represents the maximum concentration needed to reach a rate of ½ V_{max} (B) The substrate inhibition equation. The initial velocity depends on maximum velocity (V_{max}), substrate concentration ([S]), Michaelis-Menten constant (K_m), and inhibitor constant (K_i).

Substrate inhibition builds upon the assumptions used in Michaelis-Menten kinetics where the free enzyme binds the substrate to form an enzyme-substrate complex at a rate of k_1 (Figure 10). However, the concept of substrate inhibition lies in the second binding of the substrate to the enzyme-substrate complex to form SES, denying product formation. The rate of formation of SES is governed by the inhibitor constant, k_i. Therefore, the rate of ES dissociation depends on k_{-1}, k_{-2}, and k_i, unlike with Michaelis-Menten kinetics. The substrate inhibition incorporates this change to account for the decrease in velocity as substrate concentration increases past a certain point (Figure 9).

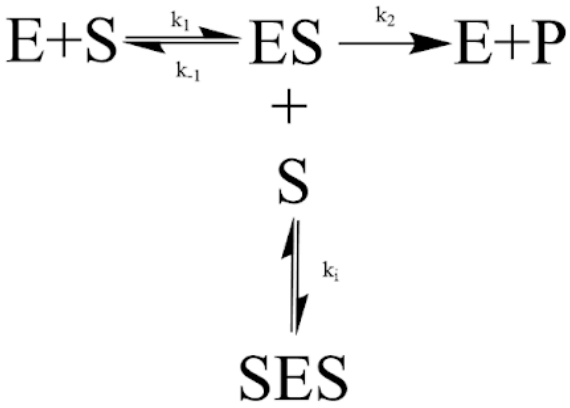

Figure 10. General reaction mechanism of an enzyme undergoing substrate inhibition. Where E represents the enzyme, S represents the substrate, and P represents the products. The previous rates of association (k_1) and the rates of dissociation (k_{-1} and k_2) are also shown. The rate of enzyme and product reverting to the enzyme substrate complex (k_{-2}) is negligible according to the first assumption. The rate of SES formation is governed by the inhibitor constant (k_i) and is assumed to form no products.

Due to the prevalence of substrate inhibition, studying its effects using a model enzyme offers some importance. AKR 163 could be this model enzyme due to its pharmaceutical potential and possible biological relevance. Furthermore, it can be used as a method to uncover what makes AKR 163 different from most of its family members when converting substrates electron-withdrawing molecules such as ethyl 4-chloroacetoacetate (E4ClAA). With this specific substrate, previous research has found that an enzyme, YDL124W, can asymmetrically reduce E4ClAA to produce ethyl (S)-4-chloro-3-hydroxybutyrate (E(S)4Cl3HB) like AKR 163 (Jung et al. 2010). However, E4ClAA causes substrate inhibition when AKR 163 reduces it but not with YDL124W (Akbary et al. 2023). Interestingly, researchers of the Cassano lab found that AKR 163 can also catalyze the reverse reaction, converting E(S)4Cl3HB to E4ClAA with no inhibition. Understanding the mechanism of action may give some insight into the relatively understudied area of substrate inhibition.

Alleviating Substrate Inhibition

Like other AKRs, AKR 163 likely exhibits a bi-bi reaction mechanism and ordered binding while utilizing a series of conformational changes (Penning 2015, Figure 11). After the enzyme binds NADPH, it undergoes one conformational change to accommodate the substrate. When the substrate binds, the enzyme changes configuration again to facilitate the hydride transfer from NADPH. Next, the enzyme changes conformation when the substrate is reduced, and the product leaves. Ultimately, the enzyme changes conformation to allow $NADP^+$ to exit. This final conformational change to release $NADP^+$ is the rate-limiting step of the enzymatic reaction (Penning 2015). The free energy change of this step is small, and it is readily reversible

(Sanli et al. 2003). For these reasons, substrate inhibition in AKR 163 would likely occur around this step; other substrate molecules would bind to the enzyme-$NADP^+$ complex since it dissociates slowly. Additionally, the rate of production of the enzyme-$NADP^+$ complex (k_9) occurs faster than the rate-limiting step (Akbary et al 2023, Figure 11). This characteristic indicates that the substrate has many opportunities to bind the enzyme-$NADP^+$ complex since it is produced quickly but breaks apart slowly. When this occurs, the enzyme would be unable to catalyze the reaction since hydride transfer cannot occur with $NADP^+$. Furthermore, less enzyme is able to be reused to perform catalysis.

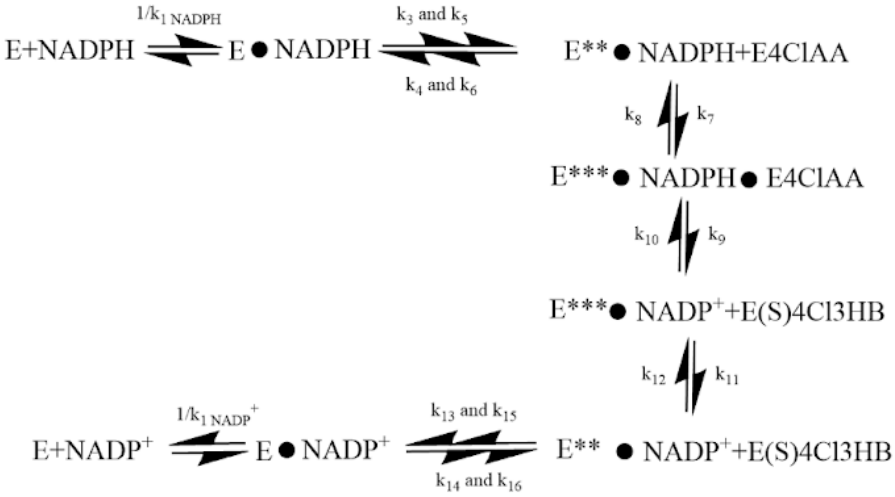

Figure 11. The bi-bi reaction scheme of AKR 163. The enzyme binds two substrates (NADPH and E4ClAA) and releases two products ($NADP^+$ and ethy (S)l 4-chloro-3-hydroxybutyrate (E(S)4Cl3HB)). Each asterisk represents a conformational change. Adapted from Cooper et al. 2007.

Enzymes often utilize electrostatic interactions, or salt bridges, between amino acids to perform their function (Penning 2015). Aldo-keto reductases are no exception (Sanli et al. 2003). In many enzymes within the superfamily, the Rosmann folds bind the nicotinamide ring of NADPH using these interactions (Wilson et al. 1993). When NADPH is docked within

the enzyme, other salt bridge interactions allow the substrate to bind. Dr. Cassano confirmed these interactions in the enzyme-NADPH complex are also within the enzyme-$NADP^+$ complex through sequence alignments.

Non-covalent bonds like salt bridge interactions likely govern the enzyme's structure as well as its conformational changes. Changing these salt bridges may increase or decrease the rates of conformational changes and potentially alleviate substrate inhibition. Additionally, altering salt bridge interactions could alleviate substrate inhibition by disrupting the substrate binding to the enzyme-$NADP^+$ complex. Therefore, alleviating substrate inhibition in Aldo-Keto reductase 163 would require some way to alter salt bridge interactions. Two ways to do this would be: (1) changing the protonation state of amino acids involved in salt bridge formation or (2) adding foreign ions to disrupt electrostatic interactions within the enzyme. Both methods likely involve the increase of ionic strength in solution. Previous researchers in the Cassano lab studied both of these ideas individually. Ivelisse Lorenzo, Honglin Yu, Karyme Paez, and Narisa Lee studied the effects of pH on substrate inhibition. They found that electron-withdrawing groups on substrates are responsible for inhibition, and lowering pH alleviates it. However, their results bear some uncertainty since they used a two-buffer system to obtain their pH range. Meanwhile, Gabby Tronosky studied the effects of salt ions on substrate inhibition. She found that increasing the concentration of salt ions decreased substrate inhibition in AKR 163. However, her project focused on one specific pH value. For my project, I will be combining these two ideas to observe the effects of pH and salt ions together on substrate inhibition regarding E4ClAA and AKR 163. Additionally, I will use a single buffer system for each pH

value for more consistent results. With these changes, I hope to uncover the effects of pH and salt ions together on enzyme catalysis and K_m/K_i.

Methods

Enzyme Purification and Production

Enzyme purification and production for these experiments were adapted from Akbary and her colleagues. Chemicals used for enzyme purification and production were obtained from Sigma Aldrich. Overnight cultures were made using 25 µL of a glycerol stock containing bacteria with the AKR 163 expression vector to 25 mL of LB media (1% glycerol, 5 mg/L kanamycin). These cultures were incubated at 30 ◦C and 200 rpm. To 500 mL of media, 10 mL of the overnight culture was added and incubated at 30 ◦C and 200 rpm. When OD_{400} reached 0.4-0.5, 0.5 mM of IPTG was added to induce gene expression while the cultures continued growing for 3 to 4 hours. The bacteria were collected and washed with wash buffer (125 mM Tris, 150 mM NaCl, pH 8.0). These pelleted cells were stored at -80 ◦C until purification.

The pellets were lysed with Bacterial Protein Extraction Reagent (B-PER, ThermoScientific) using the manufacturer's procedure and centrifuged. The lysate was combined with an equal volume of wash buffer and applied to a 10 mL column of Pierce™ Glutathione Superflow Agarose (ThermoScientific) previously equilibrated with the same buffer. Affinity purification was performed using the manufacturer's procedure. Glutathione in the elution pool was removed using Pierce™ Protein Concentrators (ThermoScientific) with wash buffer. The final

concentrations of AKR 163 fusion proteins were determined by A280 using a calculated molar extinction coefficient of 90,190 $\frac{Abs}{M \bullet cm}$ based on the number of tryptophan and tyrosine residues in the primary sequence. The enzyme solutions were stored at -20 ◦C.

Buffer Production

For the experiments at varying pHs, 0.055M ACES (pKa ~ 6.8) was made. This solution was aliquoted into three 250 mL bottles. The starting pH was measured to be 4.5 with a pH meter. The first bottled solution was filled with 1M NaOH until it reached a final pH of 6.02. The second was filled with 1M NaOH and reached a final pH of 7.00. The third was filled with 1M NaOH until it reached a final pH of 8.00. These buffers were stored and used at room temperature.

Measuring the effect of pH on enzyme kinetics

Serial dilutions of E4ClAA were done in DMSO to obtain concentrations ranging from 2 mM to 300 mM. These solutions were diluted by 50x upon addition to reaction mixtures containing pH 6, 7, or 8 ACES buffer (0.0325 mM), NADPH (100 µM), enzyme (84 nM), and Millipore water. The final volume of the reaction mixtures was 1 mL. The addition of the enzyme initiated the reactions. The reaction was monitored through the loss of NADPH over time using a Cary 60 UV-Vis spectrophotometer at an absorbance of 340 nm using the Cary WinUV Kinetics application. Microsoft excel was used to determine the initial velocity (V_0) of the reactions by using the molar extinction coefficient of NADPH (6.22 $\frac{Abs}{mM \bullet cm}$), path length (1 cm), and the

gradients of the NADPH versus time plots. The velocities were used to fit to either substrate inhibition or Michaelis-Menten plots where appropriate on KaleidaGraph™. The maximum velocity (V_{max}), Michaelis-Menten constant (K_m), and inhibitor constant (K_i) were obtained from the program as well. The V_{max} and total enzymes were used to find the catalytic power (k_{cat}). This value and the Km were used to find the catalytic efficiency.

Measuring the effect of salt concentration on enzyme kinetics

Serial dilutions of E4ClAA were done in DMSO to obtain concentrations ranging from 2 mM to 300 mM. These solutions were diluted by 50x upon addition to reaction mixtures containing pH 6, 7, or 8 ACES buffer (0.0325 mM), NADPH (100 μM), NaCl solution (1M), enzyme (0.47 nM), and Millipore water. The final volume of the reaction mixtures was 1 mL each. The reactions were used to generate absorbance versus time plots and substrate inhibition curves using previously described methods. The k_{cat} and efficiency were also calculated after data collection.

Results

As mentioned before, previous researchers have measured the effects of pH on substrate inhibition of AKR 163 with consistent results. They found that substrate inhibition decreased as pH decreased. However, they used different buffers for each pH value, which may induce some amount of systematic error. To clarify this uncertainty, the experiments were repeated with ACES buffer for each pH value (pH 6-8). This new system yielded the same results as previous studies

(Figure 12). At pH 6, the substrate inhibition curve was pronounced with an inhibition constant (K_i) value of 3.17 mM (Figure 12A). At pH 7, the substrate inhibition curve looks more defined and carries a K_i value of 1.79 mM, indicating that the inhibitor binds stronger compared to the pH 6 trial. However, at pH 8, the substrate inhibition curve is the most pronounced with a K_i value of 0.918 mM, following the trend (Figure 12C). These results provide more basis for the findings of the past experiments.

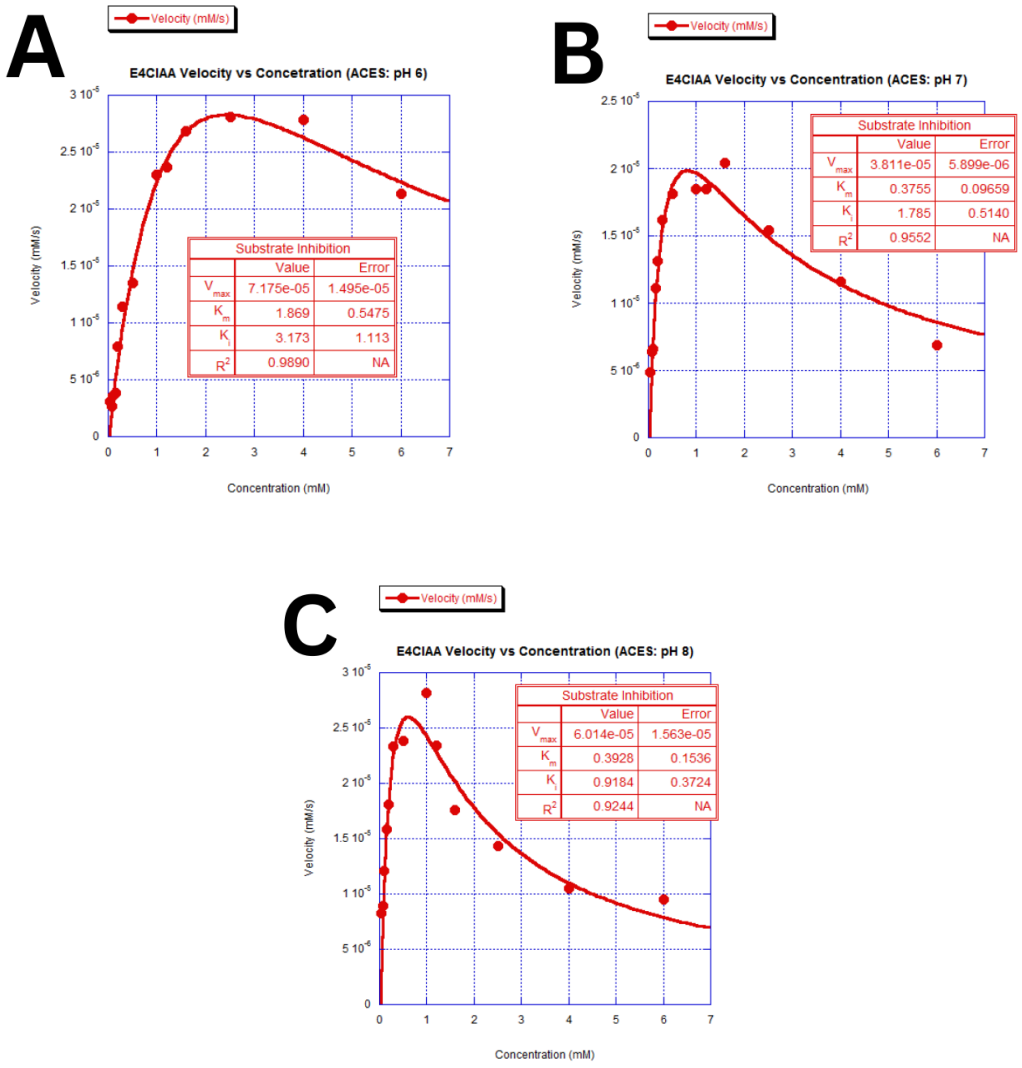

Figure 12. Substrate inhibition plots of AKR 163 with Ethyl 4-chloro-acetoacetate (E4ClAA) at different pH values. Each point represents the average of 2 trials. (A) E4ClAA reactions at pH 6. The substrate inhibition curve is less exaggerated than the other trials. Furthermore, the K_m and K_i values are also much higher. This indicates a lower binding affinity of the enzyme and substrate/inhibitor. (B) E4ClAA reactions at pH 7. The substrate inhibition curve is pronounced. This shape is due to the relatively high K_i value compared to the pH 6 trial. (C) E4ClAA reactions at pH 8. The substrate inhibition curve is much more pronounced than the other trials. Furthermore, the K_m and K_i values are lower, indicating a higher binding affinity between the enzyme and the substrate/inhibitor.

The effects of salt on AKR 163 substrate inhibition were also determined through previous experiments - adding NaCl decreased substrate inhibition. This experiment was repeated with the new ACES buffer system, confirming the previous observations (Figure 13). The pH 8 trial without salt had a K_i value of 0.9184 mM (Figure 13A). However, with 1M NaCl, the K_i value of the pH 8 trial increased substantially to 3.793 mM (Figure 13B).

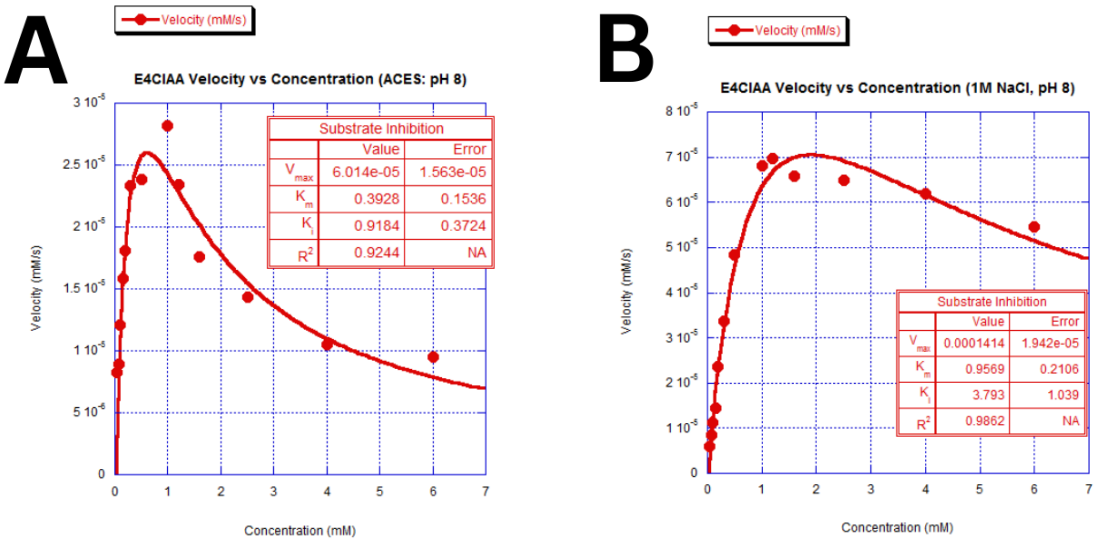

Figure 13. Differences in kinetic parameters with no NaCl and 1M NaCl at pH 8. Each point represents the average of 2 trials. (A) E4ClAA reactions at pH 8 with 0M NaCl. The substrate inhibition curve is more pronounced due to the lower magnitude of the K_i and K_m values. Furthermore, the Vmax is relatively low, which relates to a lower kcat. (B) E4ClAA reactions at pH 8 with 1M NaCl. The substrate inhibition curve is less pronounced because of the increase in the K_m and K_i. The Vmax is considerably higher in magnitude than the trials without NaCl.

Since the effects of pH and salt ions on substrate inhibition with the ACES buffer system were determined to be consistent with prior findings, the next step was to combine the two ideas to determine their effect on substrate inhibition. I reasoned that with decreasing pH and increasing salt, the inhibition would decrease. At the lowest pH with 1M NaCl, the shape of the

plot mostly resembled a Michaelis-Menten curve (Figure 14A). It was difficult to determine whether this trial followed Michaelis-Menten kinetics or substrate inhibition kinetics due to its curvature and the similar correlation coefficient (R^2) values. However, substrate inhibition likely still occurs as the K_i value for this trial was 6.770 mM. The pH 7 trial showed more inhibition as the K_i value decreased to 1.507 mM, and the shape of the inhibition curve was more pronounced (Figure 14B). However, unlike our predictions, the pH 8 trial closely resembles the pH 7 trial, instead of being more inhibited (Figure 14C). Furthermore, the K_i for this trial was 3.793 mM, much larger than the pH 7 trial. These results show a direct decrease in inhibition when looking at pH 6 and 8. However, the K_i values from pH 6 to 8 do not show any clear trends and should not be the only characteristics used to assess the impact of substrate inhibition.

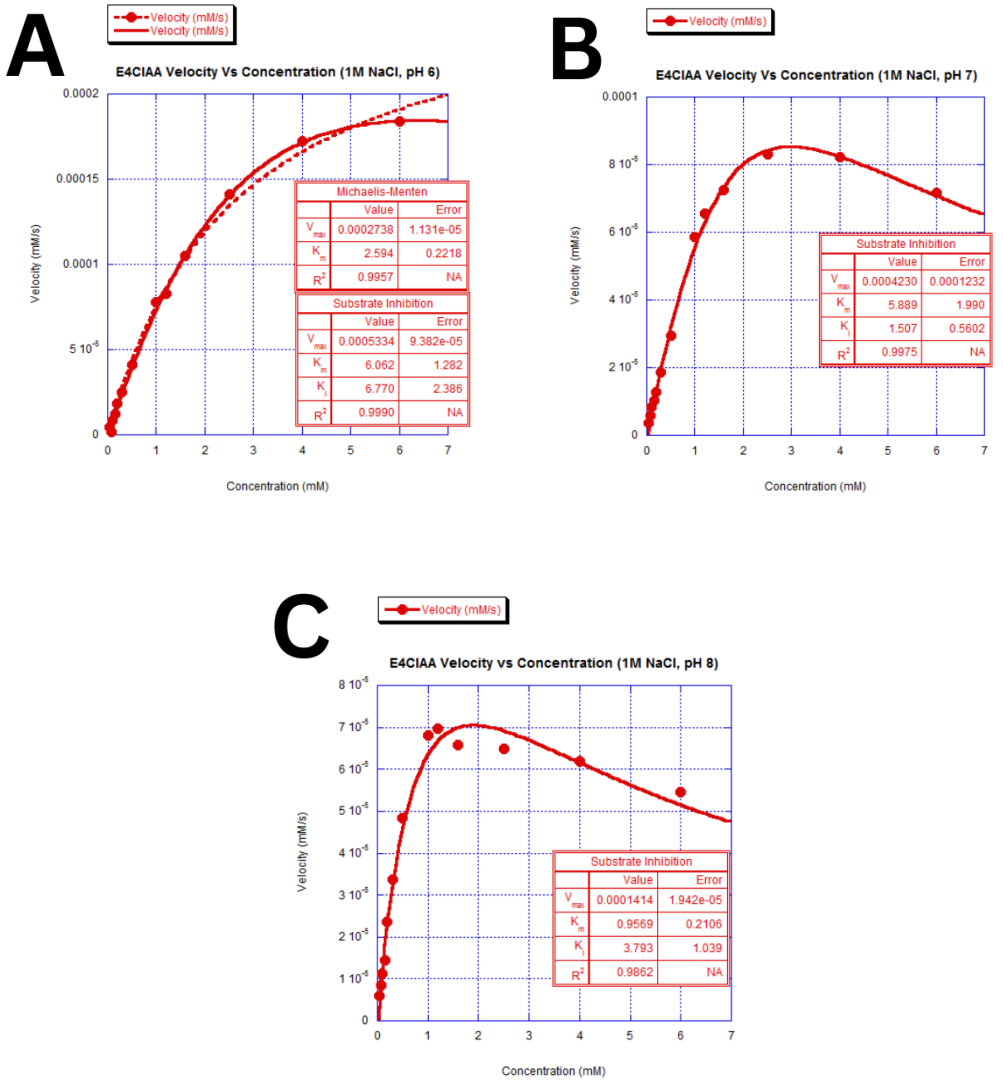

Figure 14. Substrate inhibition plot of AKR 163 with E4ClAA at pH 6, 7, and 8 with 1M NaCl. Each point represents the average of 2 trials. (A) E4ClAA reactions at pH 6 and 1M NaCl. This curve was fitted to Michaelis-Menten and substrate inhibition equations. Substrate inhibition is alleviated up to 6 mM of E4ClAA. The K_m and V_{max} values are larger than the other trials with NaCl. The K_i value is higher, but the associated error makes this aspect unreliable. (B) E4ClAA reactions at pH 7 and 1M NaCl. The V_{max} and K_m values are lower than the pH 6 trials, but noticeably higher than the pH 8 trials. The inhibitor constant for this trial is the lowest, suggesting that the salt impacts substrate binding to the enzyme-NADPH complex more than the substrate binding to the enzyme-$NADP^+$ complex. (C) E4ClAA reactions at pH 8 and 1M NaCl. These results confirm that lower K_m and K_i are associated with more substrate inhibition.

In addition to K_i, other values and trends can potentially highlight differences in substrate inhibition for each of the trials in Figure 14. For example, the K_m values decrease from pH 6 to pH 8, indicating better substrate binding affinity (Figure 14). Since the inhibitor and the substrate are theorized to be the same species (E4ClAA), changes in K_m could be directly related to the inhibitor's ability to bind as well. The enzyme's catalytic power (k_{cat}) also decreases as the pH decreases from pH 6 to 8 with 1M NaCl (Table 1). The high k_{cat} of pH 6 could indicate that the presence of salt increases the velocity of a reaction, helping the enzyme overcome substrate inhibition. Despite uncertainties, these characteristics may provide more insight into the alleviation of substrate inhibition regardless of the unprecedented K_i values in Figure 14.

Table 1

Comparison of the kinetic parameters of the different reactions.

Conditions	V_{max} (mM/s)	K_m (mM)	K_i (mM)	k_{cat} (s^{-1})	Efficiency ($\frac{s^{-1}}{mM}$)
pH 6 No NaCl	$7.18 \times 10^{-5} \mp 1.50 \times 10^{-5}$*	1.87 ∓ 0.5475	3.17 ∓ 1.11	0.854	0.457
pH 7 No NaCl	$3.81 \times 10^{-5} \mp 5.90 \times 10^{-6}$	0.376 ∓ 0.09659	1.79 ∓ 0.514	0.454	1.21
pH 8 No NaCl	$6.01 \times 10^{-5} \mp 1.56 \times 10^{-5}$	0.393 ∓ 0.1536	0.918 ∓ 0.372	0.716	1.82
pH 6 1M NaCl (MM curve)	$2.74 \times 10^{-4} \mp 1.13 \times 10^{-5}$	2.59 ∓ 0.221	___	3.26	1.26
pH 6 1M NaCl (SI curve)	$5.33 \times 10^{-4} \mp 9.38 \times 10^{-5}$	6.06 ∓ 1.28	6.77 ∓ 2.39	6.35	1.05
pH 7 1M NaCl	$4.23 \times 10^{-4} \mp 1.23 \times 10^{-4}$	5.89 ∓ 1.99	1.51 ∓ 0.560	5.04	0.855
pH 8, 1M NaCl	$1.41 \times 10^{-4} \mp 1.92 \times 10^{-5}$	0.957 ∓ 0.211	3.79 ∓ 1.04	1.68	1.76

*Error values generated from how accurately the data points align with the KaleidaGraph™ fits.

Discussion

Previous researchers have studied various aspects of Aldo-keto reductases. These findings include the tendency of electron-withdrawing substrates to induce substrate inhibition (Akbary et al. 2023), lowering pH decreases substrate inhibition (Lee 2023), and increasing salt concentrations also decreases inhibition (Tronosky 2023). Despite the variety of researchers, many characteristics of AKR 163 are still unknown and understanding how it works requires many assumptions. For instance, the specific molecular interactions that govern substrate binding and catalysis are not well understood. Additionally, the catalytic tetrad, ordered binding mechanism, and many other aspects of catalysis are based on conserved traits within the AKR superfamily and not on studies of AKR 163 itself. Nonetheless, this study aims to start building on ideas constructed by previous researchers by observing the effects of salt and pH together on the electron-withdrawing substrate ethyl 4-chloroacetoacetate (E4ClAA).

Effect of pH on Substrate Inhibition

The first few experiments of my research aimed to confirm the validity of the effects of pH on substrate inhibition using a single buffer system to verify previous research. In this regard, I hypothesized that lowering pH decreases substrate inhibition by affecting amino acid protonation states and salt bridge interactions within the enzyme. This idea was based on pH changes affecting the protonation states of amino acids in the enzyme's binding pocket or catalytic site (Radha Kishan et al. 2001). Unsurprisingly, decreasing pH for these reactions decreased substrate inhibition (Figure 12). K_m and K_i increased as substrate inhibition decreased

(Table 1) which gives some insight into E4ClAA binding the enzyme-NADPH complex and the enzyme-$NADP^+$ complex respectively. The increase in these values at lower pHs could be explained by the proposed differences in the protonation states of specific residues responsible for the enzyme binding NADPH or the substrate; by altering the protonation state, the enzyme may become less likely to bind the substrate, decreasing the likelihood of substrate inhibition. More data or insight into the mechanisms of the enzyme's binding interactions with NADPH and/or the substrate would help solidify this hypothesis.

Effect of Salt Ions on Substrate Inhibition

In addition to pH, the presence of ions was also hypothesized to affect the activity of AKRs due to their effect on salt bridges; they can interfere with these interactions. The next experiments were performed to confirm this assessment. As expected, adding 1M NaCl relieves substrate inhibition (Figure 13). Gabby Tronosky also obtained similar findings at pH 8 (Tronosky 2023). Similar to pH, K_m, and K_i generally increased as substrate inhibition decreased (Table 1). Additionally, catalytic power (k_{cat}) also increased as the pH decreased only when salt was added (Figure 15).

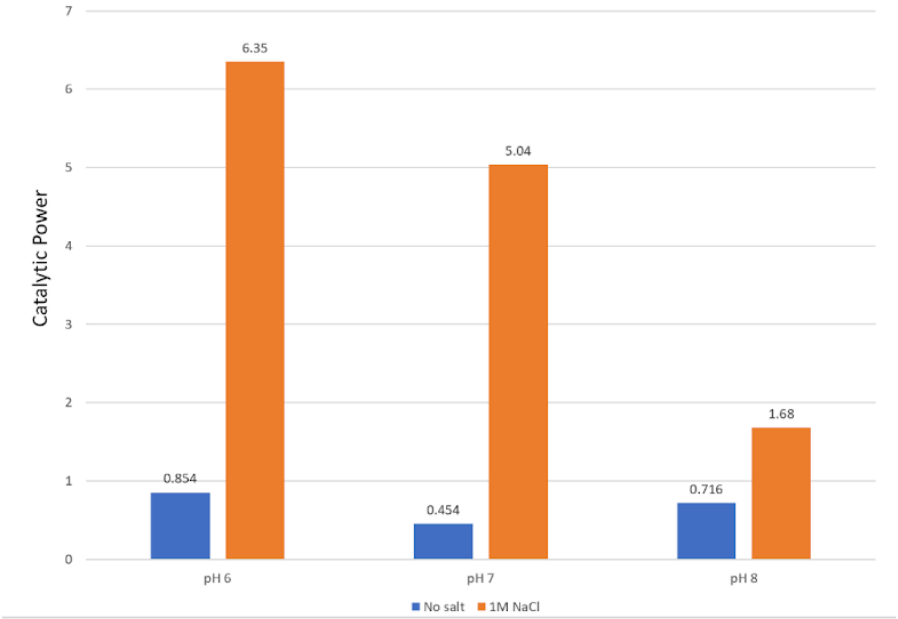

Figure 15. Comparisons of the catalytic power (k_{cat}) at different pHs with and without salt.

The k_{cat} increases when pH decreases in the presence of salt (Figure 15), suggesting that catalysis increases. Any changes to the enzyme's catalytic activity would likely be due to an increase in the speed of the $NADP^+$ dissociation step (Tronosky 2023, Akbary et al. 2023). When the rate of this step increases, it indicates that more free enzyme is ready for catalysis since $NADP^+$ exits faster. This phenomenon likely occurs due to an increase in the solution's ionic strength which speeds up the rates of conformational changes. This idea is supported by the fact that pH alone does not result in noticeable changes in k_{cat} due to its low effect on ionic strength. However, salt and pH together results in a stronger ionic strength and leads to an observable change in k_{cat}.

Separately, another potential for increase in k_{cat} could be due to the increase in enzyme catalysis. Previous studies have elucidated the conserved catalytic tetrad of AKRs - tyrosine (Tyr), histidine (His), aspartic acid (Asp), and lysine (Lys) (Jez et al. 1997). The tyrosine residue

forms salt bridges with other catalytic residues to facilitate acid-base catalysis. According to Schlegel and their colleagues, the catalytic tyrosine residue was noted to be in its most protonated form in the reduction direction of AKR1C9 catalysis. This feature was also elucidated as a part of the general mechanism of catalysis of AKRs by Barski and their colleagues (Figure 5). Assuming these models apply to AKR 163, lower pHs would favor this version of tyrosine, which could begin to explain an increase in catalytic strength at pH 6 compared to pH 8. However, this reason is not as viable as the first since it does not account for the vast differences between trials with and without salt.

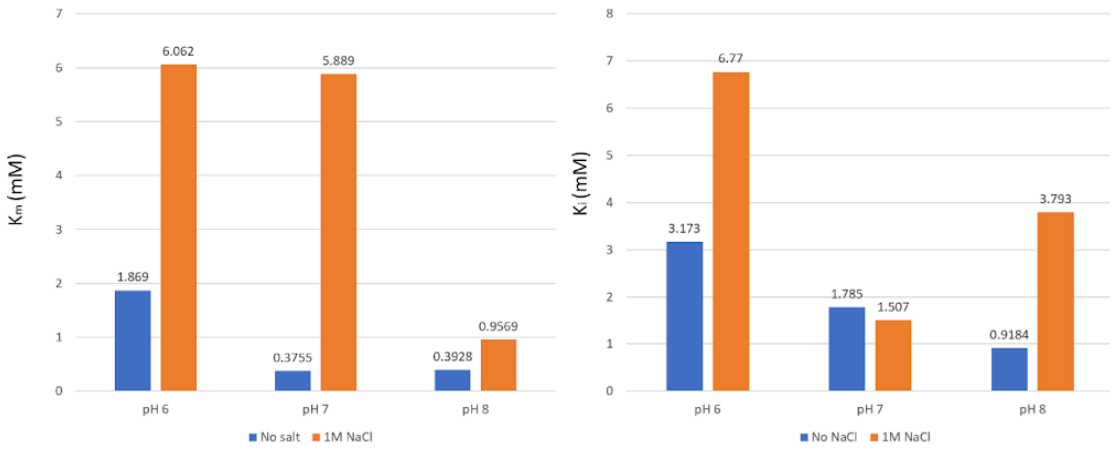

Figure 16. Comparisons of the Michaelis-Menten constant (K_M) and inhibitor constant (K_i) at different pHs with and without salt.

Similarly, K_m and K_i generally increase under these conditions (Figure 16). This feature is likely due to the predicted impact of the relative environment on salt bridges necessary to maintain stable binding (Pylaeva et al. 2018). As with k_{cat}, adding exogenous ions into the solution would increase its ionic strength which could lead to the destabilization of substrate or NADPH/$NADP^+$ binding. If salt bridges that make up the binding site have weakened or altered interactions, that would result in an increased K_m, since the enzyme has a lessened affinity for the

substrate. Furthermore, if the enzyme-NADPH complex is comparable to the enzyme-$NADP^+$ complex, the K_i would also increase since the substrate would bind with less affinity to the enzyme-$NADP^+$ complex as well.

Adding salt ions along with pH show clear trends with k_{cat} (Figure 15), K_i/K_m (Figure 16), and alleviating substrate inhibition with up to 6 mM of substrate (Figure 14A). This phenomenon is likely due to the increase in ionic strength of the solution. That is, for the enzyme to have increased catalytic activity with a simultaneous decrease in substrate/cofactor binding affinity, there is likely to be a change in the overall structure of the enzyme due to alterations in electrostatic interactions. To explain these concurrent effects, I believe that changes in the ionic strength of the solution increases the rate of conformational changes within the enzyme which destabilizes substrate/cofactor binding, but increases $NADP^+$ dissociation. Similar to my hypothesis, Gabby Tronosky also mentioned that the rate-limiting step ($NADP^+$ release) increased as ionic strength increased (Tronosky 2023). This idea fits into the proposed explanation since the enzyme likely undergoes structural changes that allow $NADP^+$ to be released more quickly, increasing K_i (binding destabilization) and even V_{max}/k_{cat} (catalytic activity increase). My current experiments are unable to directly prove these ideas with absolute certainty. However, future experiments can also provide insight into this phenomenon.

Relationship Between K_i and K_m in Substrate Inhibition

In this case of substrate inhibition, the Michaelis-Menten constant (K_m) represents the substrate binding to the enzyme-NADPH complex while the inhibition constant (K_i) represents

the substrate binding to the enzyme-$NADP^+$ complex. Given their similarities, K_m and K_i are likely closely related (Figure 16). Generally, this relatedness is expected as the substrate inhibition equation (Haldane equation) is based on the notion that K_m is the minimum concentration of substrate required to reach ½ V_{max} while K_i is the maximum substrate concentration required to reach ½ V_{max} when unbound substrate concentration is zero (Haldane 1965; Stark and Firestone 1996; Koper et. al 2010). Therefore, as K_m increases, K_i is also expected to increase and vice versa. This trend is seen in the results (Table 1) - usually K_i is larger than K_m, and when either one increases, the other also increases. This trend also supports the idea that the enzyme-NADPH and enzyme-$NADP^+$ complexes are comparable to each other as they likely utilize similar mechanisms to bind the substrate. If decreasing the pH and adding salt decreases stabilizing interactions between the substrate and the enzyme-$NADP^+$ complex, it would affect the association of the substrate and enzyme-NADPH complex.

This phenomenon can be problematic as increasing the K_m could likely affect the substrate's ability to bind the enzyme-NADPH complex which is necessary for catalysis. However, when K_i approaches infinity, substrate inhibition becomes more alleviated and the plot begins to resemble a typical Michaelis-Menten curve as seen in Figure 14A (Papácek et al. 2007). This characteristic means that alleviating substrate inhibition only requires K_i to be a substantially large value compared to K_m , which is generally possible since K_m will usually be lower than K_i. However, a large K_m value is generally indicative of a larger k_{cat} value due to its relationship with K_{sp} and efficiency, which is generally desirable (Bauer et al. 2001).

Conclusion

Generally, Aldo-Keto reductases (AKRs) experience typical Michaelis-Menten kinetics where the velocity increases to a maximum as substrate concentration increases. However, a novel AKR, Aldo-Keto Reductase 163 (AKR 163), experiences substrate inhibition in the presence of electron-withdrawing substrates. This phenomenon was alleviated by adding decreasing pH and/or adding 1M NaCl to the solutions. Kinetic parameters such as K_m, K_i, and k_{cat} generally increased as inhibition decreased. Specifically, the catalytic power at pH 6 with 1M NaCl was nine times greater than at pH 8 without salt. Furthermore, the K_m was 15 times greater and the K_i was seven times higher at pH 6 with 1M NaCl than at pH 8 without salt. These characteristics suggest that changes in pH and addition of salt affects the ionic strength of the solution which alters the enzyme's structure, leading to substrate binding destabilization and a simultaneous increase in catalytic activity.

While it was easy to observe the alleviation of substrate inhibition through plots, it is more complex to give specific explanations of the molecular events that give rise to this phenotype. The current hypothesis is that decreasing pH and increasing salt alters the conformational changes involved with cofactor binding, leading to a lower percentage of the enzyme in a form that can bind the substrate. Such a circumstance would lead to the high K_M and K_i values observed. This hypothesis predicts that the K_M for the NADPH cofactor should also increase under these conditions. Future experiments should also look into modeling the structure of AKR 163 to better understand these happenings. Additionally, observing the effects of

different salts at more diverse concentrations could also begin to explain the exact mechanism behind the effects of ionic strength and pH.

References

Abedin, Z.; Sen, S.; Field, J. Aldo-Keto Reductases Protect Lung Adenocarcinoma Cells from the Acute Toxicity of B[A]P-7,8-Trans-Dihydrodiol. *Chemical Research in Toxicology* 2011, *25* (1), 113–121. https://doi.org/10.1021/tx200272v.

Adler-Nissen, J. Limited Enzymic Degradation of Proteins: A New Approach in the Industrial Application of Hydrolases. *Journal of Chemical Technology and Biotechnology* 2007, *32* (1), 138–156. https://doi.org/10.1002/jctb.5030320118.

Akbary, Z.; Yu, H.; Lorenzo, I.; Paez, K.; Lee, N. D.; DeBeVoise, K.; Moses, J.; Sanders, N.; Connors, N.; Cassano, A. Electron Withdrawing Group-Dependent Substrate Inhibition of an α-Ketoamide Reductase from Saccharomyces Cerevisiae. *Biochem. Biophys. Res. Commun.* 2023, *676*, 97–102. https://doi.org/10.1016/j.bbrc.2023.07.030.

Barski, O. A.; Tipparaju, S. M.; Bhatnagar, A. The Aldo-Keto Reductase Superfamily and Its Role in Drug Metabolism and Detoxification. *Drug Metabolism Reviews* 2008, *40* (4), 553–624. https://doi.org/10.1080/03602530802431439.

Bell, E. L.; Finnigan, W.; France, S. P.; Green, A. P.; Hayes, M. A.; Hepworth, L. J.; Lovelock, S. L.; Niikura, H.; Osuna, S.; Romero, E.; Ryan, K. S.; Turner, N. J.; Flitsch, S. L. Biocatalysis. *Nature Reviews Methods Primers* 2021, *1* (1), 1–21. https://doi.org/10.1038/s43586-021-00044-z.

Bauer, C.; Osman, A. M.; Cercignani, G.; Gialluca, N.; Paolini, M. A Unified Theory of Enzyme Kinetics Based upon the Systematic Analysis of the Variations of Kcat, KM, and Kcat/KM and the Relevant ΔG0≠ Values—Possible Implications in Chemotherapy and Biotechnology.

Biochemical Pharmacology 2001, *61* (9), 1049–1055. https://doi.org/10.1016/s0006-2952(01)00579-2.

Blaber, M. 7.2: Derivation of Michaelis-Menten Equation. https://bio.libretexts.org/Courses/Wheaton_College_Massachusetts/Principles_of_Biochemistry/07%3A_Enzymes_catalysis_and_kinetics/7.02%3A_Derivation_of_Michaelis-Menten_equation (accessed 2024-01-10).

Bohren, K. M.; Grimshaw, C. E.; Lai, C.-J.; Harrison, D. G.; Ringe, D.; Petsko, G. A.; Gabbay, K. H. Tyrosine-48 Is the Proton Donor and Histidine-110 Directs Substrate Stereochemical Selectivity in the Reduction Reaction of Human Aldose Reductase: Enzyme Kinetics and Crystal Structure of the Y48H Mutant Enzyme. *Biochemistry* 1994, *33* (8), 2021–2032. https://doi.org/10.1021/bi00174a007.

Bokel, A; Rühlmann, A; Hutte, M.C.; Urlacher, V. B. Enzyme-Mediated Two-Step Regio- and Stereoselective Synthesis of Potential Rapid-Acting Antidepressant (2*S*,6*S*)-Hydroxynorketamine. *ACS Catalysis* 2020, *10* (7), 4151–4159. https://doi.org/10.1021/acscatal.9b05384.

Calam, E.; Porté, S.; Fernández, M. R.; Farrés, J.; Parés, X.; Biosca, J. A. Biocatalytic Production of Alpha-Hydroxy Ketones and Vicinal Diols by Yeast and Human Aldo–Keto Reductases. *Chemico-Biological Interactions* 2013, *202* (1-3), 195–203. https://doi.org/10.1016/j.cbi.2012.12.006.

Chang, K.-C.; Laffin, B.; Ponder, J.; Énzsöly, A.; János Németh; LaBarbera, D. V.; J. Mark Petrash. Beta-Glucogallin Reduces the Expression of Lipopolysaccharide-Induced Inflammatory

Markers by Inhibition of Aldose Reductase in Murine Macrophages and Ocular Tissues. *Chemico-biological interactions (Print)* 2013, *202* (1-3), 283–287. https://doi.org/10.1016/j.cbi.2012.12.001.

Chen, J.; Ma, Q.; Li, M.; Chao, D.; Huang, L.; Wu, W.; Fang, Y.; Dong, S. Glucose-Oxidase like Catalytic Mechanism of Noble Metal Nanozymes. *Nature Communications* 2021, *12* (1). https://doi.org/10.1038/s41467-021-23737-1.

Chen, M.; Jin, Y.; Penning, T. M. The Rate-Determining Steps of Aldo–Keto Reductases (AKRs), a Study on Human Steroid 5β-Reductase (AKR1D1). *Chemico-Biological Interactions* 2015, *234*, 360–365. https://doi.org/10.1016/j.cbi.2014.12.004.

Chen, W.-D.; Zhang, Y. Regulation of Aldo–Keto Reductases in Human Diseases. *Frontiers in Pharmacology* 2012, *3*. https://doi.org/10.3389/fphar.2012.00035.

Cooper, G. M. In *The cell: A molecular approach. 2nd edition*; Sinauer Associates, Inc, 2000; pp 41–89.

Cooper, W. C.; Jin, Y.; Penning, T. M. Elucidation of a Complete Kinetic Mechanism for a Mammalian Hydroxysteroid Dehydrogenase (HSD) and Identification of All Enzyme Forms on the Reaction Coordinate. *Journal of Biological Chemistry* 2007, *282* (46), 33484–33493. DOI:10.1074/jbc.m703414200.

Cornish-Bowden, A. The Origins of Enzyme Kinetics. *FEBS Letters* 2013, *587* (17), 2725–2730. https://doi.org/10.1016/j.febslet.2013.06.009.

Dydio, P; Key, H. M.; Hayashi, H.; Clark, D.; Hartwig, J. F. Chemoselective, Enzymatic C–H Bond Amination Catalyzed by a Cytochrome P450 Containing an Ir(Me)-PIX Cofactor. *Journal of the American Chemical Society* 2017, *139* (5), 1750–1753. https://doi.org/10.1021/jacs.6b11410.

Gabbay, K. H. Hyperglycemia, Polyol Metabolism, and Complications of Diabetes Mellitus. *Annual Review of Medicine* 1975, *26* (1), 521–536. https://doi.org/10.1146/annurev.me.26.020175.002513.

Ellis, E. M. Microbial Aldo-Keto Reductases. *FEMS Microbiology Letters* 2002, *216* (2), 123–131. https://doi.org/10.1111/j.1574-6968.2002.tb11425.x.

Espina, G.; Atalah, J.; Blamey, J. M. Extremophilic Oxidoreductases for the Industry: Five Successful Examples with Promising Projections. *Frontiers in bioengineering and biotechnology* 2021, *9*, 710035. https://doi.org/10.3389/fbioe.2021.710035.

Grimshaw, C. E. Aldose Reductase: Model for a New Paradigm of Enzymic Perfection in Detoxification Catalysts. *Biochemistry* 1992, *31* (42), 10139–10145. https://doi.org/10.1021/bi00157a001.

Grimshaw, C. E.; Bohren, K. M.; Lai, C.-J.; Gabbay, K. H. Human Aldose Reductase: PK of Tyrosine 48 Reveals the Preferred Ionization State for Catalysis and Inhibition. *Biochemistry* 1995, *34* (44), 14374–14384. https://doi.org/10.1021/bi00044a014.

Grimshaw, C. E.; Bohren, K. M.; Lai, C.-J.; Gabbay, K. H. Human Aldose Reductase: Rate Constants for a Mechanism Including Interconversion of Ternary Complexes by Recombinant

Wild-Type Enzyme. *Biochemistry* 1995, *34* (44), 14356–14365. https://doi.org/10.1021/bi00044a012.

Haldane JBS (1965) Enzymes. The MIT Press, Cambridge, MA.

Han, S.; Eul Soo Park; Joo Young Dong; Shin, J. Active-Site Engineering of ω-Transaminase for Production of Unnatural Amino Acids Carrying a Side Chain Bulkier than an Ethyl Substituent. *Applied and Environmental Microbiology* 2015, *81* (20), 6994–7002. https://doi.org/10.1128/aem.01533-15.

He, Y.; Tao, Z.; Zhang, X.; Yang, Z.; Xu, J. Highly Efficient Synthesis of Ethyl (S)-4-Chloro-3-Hydroxybutanoate and Its Derivatives by a Robust NADH-Dependent Reductase from E. Coli CCZU-K14. *Bioresource Technology* 2014, *161*, 461–464. https://doi.org/10.1016/j.biortech.2014.03.133.

Ikeda, S.; Okuda-Ashitaka, E.; Masu, Y.; Suzuki, T.; Watanabe, K.; Nakao, M.; Shingu, K.; Ito, S. Cloning and Characterization of Two Novel Aldo-Keto Reductases (AKR1C12 and AKR1C13) from Mouse Stomach. *FEBS Letters* 1999, *459* (3), 433–437. https://doi.org/10.1016/s0014-5793(99)01243-0.

Imada, K.; Tamura, T.; Takenaka, R.; Kobayashi, I.; Namba, K.; Inagaki, K. Structure and Quantum Chemical Analysis of NAD+-Dependent Isocitrate Dehydrogenase: Hydride Transfer and Co-Factor Specificity. *Proteins: Structure, Function, and Bioinformatics* 2007, *70* (1), 63–71. https://doi.org/10.1002/prot.21486.

Jencks, W. P. *Catalysis in Chemistry and Enzymology*; Dover Publications: New York, 1969.

Jez, J. M.; Bennett, M. J.; Schlegel, B. P.; Lewis, M.; Penning, T. M. Comparative Anatomy of the Aldo–Keto Reductase Superfamily. *Biochemical Journal* 1997, *326* (3), 625–636. https://doi.org/10.1042/bj3260625.

Johnson, K. A.; Goody, R. S. The Original Michaelis Constant: Translation of the 1913 Michaelis–Menten Paper. Biochemistry 2011, 50 (39), 8264–8269. https://doi.org/10.1021/bi201284u.

Jung, J.; Park, H. J.; Uhm, K.-N.; Kim, D.; Kim, H.-K. Asymmetric Synthesis of (S)-Ethyl-4-Chloro-3-Hydroxy Butanoate Using a Saccharomyces Cerevisiae Reductase: Enantioselectivity and Enzyme–Substrate Docking Studies. *Biochimica et Biophysica Acta (BBA) - Proteins and Proteomics* 2010, *1804* (9), 1841–1849. https://doi.org/10.1016/j.bbapap.2010.06.011.

Kang, Y.-M.; Kang, H.-A.; Cominguez, D. C.; Kim, S.-H.; An, H.-J. Papain Ameliorates Lipid Accumulation and Inflammation in High-Fat Diet-Induced Obesity Mice and 3T3-L1 Adipocytes via AMPK Activation. *International Journal of Molecular Sciences* 2021, *22* (18), 9885. https://doi.org/10.3390/ijms22189885.

Kim, T.-H.; Flick, R.; Brunzelle, J. S.; Singer, A. U.; Evdokimova, E.; Brown, G.; Jeong Chan Joo; Minasov, G.; Anderson, W. F.; Mahadevan, R.; Savchenko, A.; Yakunin, A. F. Novel Aldo-Keto Reductases for the Biocatalytic Conversion of 3-Hydroxybutanal to 1,3-Butanediol: Structural and Biochemical Studies. 2017, *83* (7). https://doi.org/10.1128/aem.03172-16.

Kokkonen, P.; Beier, A.; Mazurenko, S.; Damborsky, J.; Bednar, D.; Prokop, Z. Substrate Inhibition by the Blockage of Product Release and Its Control by Tunnel Engineering. *RSC Chemical Biology* 2021, *2* (2), 645–655. https://doi.org/10.1039/D0CB00171F.

Koper, T. E.; Stark, J. M.; Habteselassie, M. Y.; Norton, J. M. Nitrification Exhibits Haldane Kinetics in an Agricultural Soil Treated with Ammonium Sulfate or Dairy-Waste Compost. *FEMS Microbiology Ecology* 2010, *74* (2), 316–322. https://doi.org/10.1111/j.1574-6941.2010.00960.x.

Kratzer, R.; Wilson, D.; Nidetzky, B. Catalytic Mechanism and Substrate Selectivity of Aldo-Keto Reductases: Insights from Structure-Function Studies of Candida Tenuis Xylose Reductase. *IUBMB Life (International Union of Biochemistry and Molecular Biology: Life)* 2006, *58* (9), 499–507. https://doi.org/10.1080/15216540600818143.

Lan, Y.; Chen, W.; Yen, C.-C.; Chong, K.; Chen, Y.-C.; Fan, H.-C.; Chen, M.-S.; Chen, C.-M. Aldo-Keto Reductase Family 1 Member A1 (AKR1A1) Deficiency Exacerbates Alcohol-Induced Hepatic Oxidative Stress, Inflammation, Steatosis, and Fibrosis. bioRxiv (Cold Spring Harbor Laboratory) 2022. https://doi.org/10.1101/2022.12.07.519420.

Lee, ND. Investigating Substrate Inhibition and the Effects of pH in an Aldo-keto Reductase from a Yeast Strain using Electron Withdrawing Substrates. Honors Thesis, Drew University. Madison, NJ, 2023.

Lemonde, H. A.; Custard, E. J.; Bouquet, J.; Duran, M.; Overmars, H.; Scambler, P. J.; Clayton, P. T. Mutations in SRD5B1 (AKR1D1), the Gene Encoding 4-3-Oxosteroid 5 -Reductase, in

Hepatitis and Liver Failure in Infancy. *Gut* 2003, *52* (10), 1494–1499. DOI:10.1136/gut.52.10.1494.

Lewis, T.; Stone, W. L. *Biochemistry, Proteins Enzymes*. PubMed. https://www.ncbi.nlm.nih.gov/books/NBK554481/

Liu, W.; Lin, W.; Davis, A. J.; Jordán, F.; Yang, H.; Hwang, M. A Network Perspective on the Topological Importance of Enzymes and Their Phylogenetic Conservation. *BMC Bioinformatics* 2007, *8* (1). https://doi.org/10.1186/1471-2105-8-121.

Ma, H.; Ratnam, K.; Penning, T. M. Mutation of Nicotinamide Pocket Residues in Rat Liver 3α-Hydroxysteroid Dehydrogenase Reveals Different Modes of Cofactor Binding. *Biochemistry* 1999, *39* (1), 102–109. https://doi.org/10.1021/bi991659o.

Martínez, A. T.; Ruiz-Dueñas, F. J.; Camarero, S.; Serrano, A.; Linde, D.; Lund, H.; Vind, J.; Tovborg, M.; Herold-Majumdar, O. M.; Hofrichter, M.; Liers, C.; Ullrich, R.; Scheibner, K.; Sannia, G.; Piscitelli, A.; Pezzella, C.; Sener, M. E.; Kılıç, S.; van Berkel, W. J. H.; Guallar, V. Oxidoreductases on Their Way to Industrial Biotransformations. *Biotechnology Advances* 2017, *35* (6), 815–831. https://doi.org/10.1016/j.biotechadv.2017.06.003.

McGovern, P. E.; Zhang, J.; Tang, J.; Zhang, Z.; Hall, G. R.; Moreau, R. A.; Nunez, A.; Butrym, E. D.; Richards, M. P.; Wang, C. .; Cheng, G.; Zhao, Z.; Wang, C. Fermented Beverages of Pre- and Proto-Historic China. *Proceedings of the National Academy of Sciences* 2004, *101* (51), 17593–17598. https://doi.org/10.1073/pnas.0407921102.

Min, J. Y.; Lim, S.-O.; Jung, G. Downregulation of Catalase by Reactive Oxygen Species via Hypermethylation of CpG Island II on the Catalase Promoter. *FEBS Letters* 2010, *584* (11), 2427–2432. https://doi.org/10.1016/j.febslet.2010.04.048.

Mohapatra, B. R.; Bapuji, M.; Sree, A. Production of Industrial Enzymes (Amylase, Carboxymethylcellulase and Protease) by Bacteria Isolated from Marine Sedentary Organisms. *Acta Biotechnologica* 2003, *23* (1), 75–84. https://doi.org/10.1002/abio.200390011.

Monti, D.; Ottolina, G.; Carrea, G.; Riva, S. Redox Reactions Catalyzed by Isolated Enzymes. *Chemical Reviews* 2011, *111* (7), 4111–4140. https://doi.org/10.1021/cr100334x.

Ning, C.; Su, E.; Wei, D. Characterization and Identification of Three Novel Aldo–Keto Reductases from Lodderomyces Elongisporus for Reducing Ethyl 4-Chloroacetoacetate. *Archives of Biochemistry and Biophysics* 2014, *564*, 219–228. https://doi.org/10.1016/j.abb.2014.10.007.

Papácek, S; Celikovský, S; Stys, D.; Ruiz-León, JJ. Bilinear System as a Modelling Framework for Analysis of Microalgal Growth. *Kybernetika* 2007, *43* (1), 1–20.

Patil, M.; Grogan, G.; Bommarius, A.; Yun, H. Recent Advances in ω-Transaminase-Mediated Biocatalysis for the Enantioselective Synthesis of Chiral Amines. *Catalysts* 2018, *8* (7), 254. https://doi.org/10.3390/catal8070254.

Pei, R.; Jiang, W.; Fu, X.; Tian, L.; Zhou, S. 3D-Printed Aldo-Keto Reductase within Biocompatible Polymers as Catalyst for Chiral Drug Intermediate. *Chemical Engineering Journal* 2022, *429*, 132293–132293. https://doi.org/10.1016/j.cej.2021.132293.

Penning, T. M. Aldo-Keto Reductase Regulation by the Nrf2 System: Implications for Stress Response, Chemotherapy Drug Resistance, and Carcinogenesis. 2016, *30* (1), 162–176. https://doi.org/10.1021/acs.chemrestox.6b00319.

Penning, T. M. The Aldo-Keto Reductases (AKRs): Overview. *Chemico-Biological Interactions* 2015, *234*, 236–246. https://doi.org/10.1016/j.cbi.2014.09.024.

Penning, T. M.; Wangtrakuldee, P.; Auchus, R. J. Structural and Functional Biology of Aldo-Keto Reductase Steroid-Transforming Enzymes. *Endocrine Reviews* 2018, *40* (2), 447–475. https://doi.org/10.1210/er.2018-00089.

Polgár, L. The Mechanism of Action of Aspartic Proteases Involves “Push-Pull” Catalysis. *FEBS Letters* 1987, *219* (1), 1–4. https://doi.org/10.1016/0014-5793(87)81179-1.

Pollak, N.; Dölle, C.; Ziegler, M. The Power to Reduce: Pyridine Nucleotides – Small Molecules with a Multitude of Functions. *Biochemical Journal* 2007, *402* (2), 205–218. https://doi.org/10.1042/bj20061638.

Portadin, L. Product Inhibition of AKR163: an Aldoketoreductase from a Yeast Strain Recovered from Ancient Amber. Honors Thesis, Drew University. Madison, NJ, 2023.

Pylaeva, S.; Brehm, M.; Sebastiani, D. Salt Bridge in Aqueous Solution: Strong Structural Motifs but Weak Enthalpic Effect. *Scientific Reports* 2018, *8* (1), 13626. https://doi.org/10.1038/s41598-018-31935-z.

Radha Kishan K.V.; Newcomer, M. E.; Rhodes, T. H.; Guilliot, S. D. Effect of PH and Salt Bridges on Structural Assembly: Molecular Structures of the Monomer and Intertwined Dimer of

the Eps8 SH3 Domain. *Protein Science* 2001, *10* (5), 1046–1055. https://doi.org/10.1110/ps.50401.

Ramana, K. V.; Willis, M. S.; White, M.; Horton, J. W.; J. Michael DiMaio; Srivastava, D.; Bhatnagar, A. Endotoxin-Induced Cardiomyopathy and Systemic Inflammation in Mice Is Prevented by Aldose Reductase Inhibition. *Circulation* 2006, *114* (17), 1838–1846. https://doi.org/10.1161/circulationaha.106.630830.

Ranjbari, N.; Razzaghi, M.; Fernandez-Lafuente, R.; Shojaei, F.; Satari, M.; Homaei, A. Improved Features of a Highly Stable Protease from Penaeus Vannamei by Immobilization on Glutaraldehyde Activated Graphene Oxide Nanosheets. *International Journal of Biological Macromolecules* 2019, *130*, 564–572. https://doi.org/10.1016/j.ijbiomac.2019.02.163.

Rao, M. B.; Tanksale, A. M.; Ghatge, M. S.; Deshpande, V. V. Molecular and Biotechnological Aspects of Microbial Proteases. *Microbiology and Molecular Biology Reviews* 1998, *62* (3), 597–635. https://doi.org/10.1128/mmbr.62.3.597-635.1998.

Raveendran, S.; Parameswaran, B.; Ummalyma, S. B.; Abraham, A.; Mathew, A. K.; Madhavan, A.; Rebello, S.; Pandey, A. Applications of Microbial Enzymes in Food Industry. *Food Technology and Biotechnology* 2018, *56* (1). DOI:10.17113/ftb.56.01.18.5491.

Reed, M. C.; Lieb, A.; Nijhout, H. F. The Biological Significance of Substrate Inhibition: A Mechanism with Diverse Functions. *BioEssays* 2010, *32* (5), 422–429. https://doi.org/10.1002/bies.200900167.

Robinson, C. G.; Liu, Y.; Thomson, J. A.; Sturtevant, J. M.; Sligar, S. G. Energetics of Heme Binding to Native and Denatured States of Cytochrome *B*562. 1997, *36* (51), 16141–16146. https://doi.org/10.1021/bi971470h.

Sanli, G.; Dudley, J. I.; Blaber, M. Structural Biology of the Aldo-Keto Reductase Family of Enzymes: Catalysis and Cofactor Binding. *Cell Biochemistry and Biophysics* 2003, *38* (1), 79–101. https://doi.org/10.1385/cbb:38:1:79.

Schlegel, B. P.; Jez, J. M.; Penning, T. M. Mutagenesis of 3α-Hydroxysteroid Dehydrogenase Reveals a “Push−Pull” Mechanism for Proton Transfer in Aldo−Keto Reductases. *Biochemistry* 1998, *37* (10), 3538–3548. https://doi.org/10.1021/bi9723055.

Schlegel, B. P.; Ratnam, K.; Penning, T. M. Retention of NADPH-Linked Quinone Reductase Activity in an Aldo-Keto Reductase Following Mutation of the Catalytic Tyrosine†. *Biochemistry* 1998, *37* (31), 11003–11011. https://doi.org/10.1021/bi980475r.

Schmid, A.; Hollmann, F.; Park, J. B.; Bühler, B. The Use of Enzymes in the Chemical Industry in Europe. *Current Opinion in Biotechnology* 2002, *13* (4), 359–366. https://doi.org/10.1016/s0958-1669(02)00336-1.

Schwarz, G.; Mendel, R. R.; Ribbe, M. W. Molybdenum Cofactors, Enzymes and Pathways. *Nature* 2009, *460* (7257), 839–847. https://doi.org/10.1038/nature08302.

Shukla, A.; Girdhar, M.; Mohan, A. Applications of Microbial Enzymes in the Food Industry. *Food Microbial Sustainability* 2023, 173–192. DOI:10.1007/978-981-99-4784-3_9.

Sicsic, S.; Durand, P.; Langrene, S.; le Goffic, F. A New Approach for Using Cofactor Dependent Enzymes: Example of Alcohol Dehydrogenase. *FEBS Letters* 1984, *176* (2), 321–324. https://doi.org/10.1016/0014-5793(84)81188-6.

Singh, R.; Kumar, M.; Mittal, A.; Mehta, P. K. Microbial Enzymes: Industrial Progress in 21st Century. *3 Biotech* 2016, *6* (2). https://doi.org/10.1007/s13205-016-0485-8.

Souza, P. M. de; Magalhães, P. de O. e. Application of Microbial α-Amylase in Industry - a Review. *Brazilian Journal of Microbiology* 2010, *41* (4), 850–861. https://doi.org/10.1590/s1517-83822010000400004.

Stark, J. M.; Firestone, M. K. Kinetic Characteristics of Ammonium-Oxidizer Communities in a California Oak Woodland-Annual Grassland. *Soil Biology and Biochemistry* 1996, *28* (10-11), 1307–1317. https://doi.org/10.1016/s0038-0717(96)00133-2.

Tronosky, G. The Effect of Salt Ions on the Substrate Inhibition of a Novel Aldo-Keto Reductase. Honors Thesis, Drew University. Madison, NJ, 2023.

Wang, Q.; Ye, T.; Ma, Z.; Chen, R.; Xie, T.; Yin, X. Characterization and Site-Directed Mutation of a Novel Aldo–Keto Reductase from Lodderomyces Elongisporus NRRL YB-4239 with High Production Rate of Ethyl (R)-4-Chloro-3-Hydroxybutanoate. Journal of Industrial Microbiology and Biotechnology 2014, 41 (11), 1609–1616. https://doi.org/10.1007/s10295-014-1502-8.

Wilson, D. K.; Quiocho, F. A.; Bohren, K. M.; Gabbay, K. H. An unlikely sugar substrate site in the 1.65 angstroms structure of the human aldose reductase holoenzyme implicated in diabetic complications 1993. DOI:10.2210/pdb1ads/pdb.

Yagihashi, S.; Mizukami, H.; Ogasawara, S.; Yamagishi, S.-I.; Nukada, H.; Kato, N.; Hibi, C.; Chung, S.; Chung, S. The Role of the Polyol Pathway in Acute Kidney Injury Caused by Hindlimb Ischaemia in Mice. *The Journal of Pathology* 2010, *220* (5), 530–541. https://doi.org/10.1002/path.2671.

Yamamoto, K.; Wilson, D. K. Identification, Characterization, and Crystal Structure of an Aldo–Keto Reductase (AKR2E4) from the Silkworm Bombyx Mori. *Archives of Biochemistry and Biophysics* 2013, *538* (2), 156–163. https://doi.org/10.1016/j.abb.2013.08.018.

Yoshino, M.; Murakami, K. Analysis of the Substrate Inhibition of Complete and Partial Types. *SpringerPlus* 2015, *4* (1). https://doi.org/10.1186/s40064-015-1082-8.